4.5

UPDATE ON COSPA STORM FORECASTS*

H. Iskenderian†, C. Reiche, W. Dupree, M. Wolfson, T. Langlois, D. Morse, X. Tao, K. Haas, L. Bickmeier, P. Lamey, J. Pelagatti, and D. Moradi
MIT Lincoln Laboratory, Lexington, MA

J. Pinto, J. Williams, D. Ahijevych, and M. Steiner
National Center for Atmospheric Research

S. Weygandt, C. Alexander, S. Benjamin
NOAA ESRL Global Systems Division, Boulder, CO

J. Mecikalski
University of Alabama in Huntsville, AL

W. Feltz
University of Wisconsin-Cooperative Institute for Meteorological Satellite Studies, Madison, WI

K. Bedka
NASA-Langley Research Center, Hampton, VA

1. INTRODUCTION

Air traffic congestion caused by convective weather in the US has become a serious national problem. Several studies have shown that there is a critical need for timely, reliable and high quality forecasts of precipitation and echo tops with forecast time horizons of up to 12 hours in order to predict airspace capacity (Robinson et al. 2008, Evans et al. 2006 and FAA REDAC Report 2007). Yet there are currently several forecast systems available to strategic planners across the National Airspace System (NAS) that are not fully meeting Air Traffic Management (ATM) needs. Furthermore, the use of many forecasting systems increases the potential for conflicting information in the planning process, which can cause situational awareness problems during operational coordination.

A collaboration among MIT Lincoln Laboratory (MIT LL), the National Center for Atmospheric Research (NCAR) Research Applications Laboratory (RAL), and the National Oceanic and Atmospheric Administration (NOAA) Earth Systems Research Laboratory (ESRL) Global Systems Division (GSD) is developing a CONUS-scale 0-8 hour forecast capability called CoSPA (Wolfson et al. 2008). The on-going collaboration is structured to leverage the expertise and technologies of the three laboratories to build a CoSPA forecast capability that not only exceeds all current operational forecast capabilities and skill, but also provides enough resolution and skill to meet the demands of the envisioned NextGen decision support technology. The current CoSPA prototype for 0-8 hour forecasts is funded under the FAA's Aviation Weather Research Program (AWRP).

Historically, forecasts based on heuristics and extrapolation have performed well in the 0-2 hour window, whereas forecasts based on Numerical Weather Prediction (NWP) models

*This work was sponsored by the Federal Aviation Administration under Air Force Contract No. FA8721-05-C-0002. Opinions, interpretations, conclusions, and recommendations are those of the authors and are not necessarily endorsed by the United States Government. This research is in response to requirements and funding by the Federal Aviation Administration (FAA). The views expressed are those of the authors and do not necessarily represent the official policy or position of the FAA.

†*Corresponding author address*: Haig Iskenderian, MIT Lincoln Laboratory, 244 Wood Street, Lexington, MA 02420-9185; e-mail: haig@ll.mit.edu

have shown better performance than heuristics beyond 3-4 hours. One of the goals of CoSPA is to optimally blend heuristics and NWP models into a unified set of aviation-specific storm forecast products with the best overall performance possible.

CoSPA underwent an evaluation period during the summers of 2008, 2009, and 2010. After each evaluation, the collaborating laboratories made enhancements to the forecast to correct noted deficiencies. This paper discusses the updates that were made to the CoSPA system in response to the 2010 evaluation in preparation for a fourth evaluation period that began on 1 June 2011.

2. SYSTEM ARCHITECTURE

A data flow diagram for CoSPA is shown in Figure 1. A variety of meteorological data is utilized by the forecast system for the heuristic forecasting part and the NWP models. The analysis and short-term tracking and extrapolation (i.e., heuristic) aspects of the CoSPA forecast system are handled by Corridor Integrated Weather System (CIWS; Wolfson and Clark 2006) and CoSPA extrapolation at MIT LL, while NOAA's ESRL/GSD is providing the 0-15 hour High Resolution Rapid Refresh (HRRR; Smith et al. 2008) model forecasts. The heuristic extrapolation forecasts and model predictions are blended at NCAR/RAL to generate seamless 0-8 hour CoSPA forecasts of Vertically-Integrated Liquid (VIL) and Echo Tops (ET) with a 15 min granularity and 15 min update frequency. The blended forecast data are sent back to MIT LL for post-processing and display on CoSPA Situational Display stations and website (cospa.wx.ll.mit.edu).

The CoSPA display provides visualization of a variety of data relevant for understanding the current weather conditions, including satellite imagery, lightning data, and mosaics of VIL and ET derived from the NEXRAD WSR-88D radar network. A complete description of the display functionality can be found in Dupree et al. (2009a). The user can display storm motion, growth and decay trends, and verification contours.

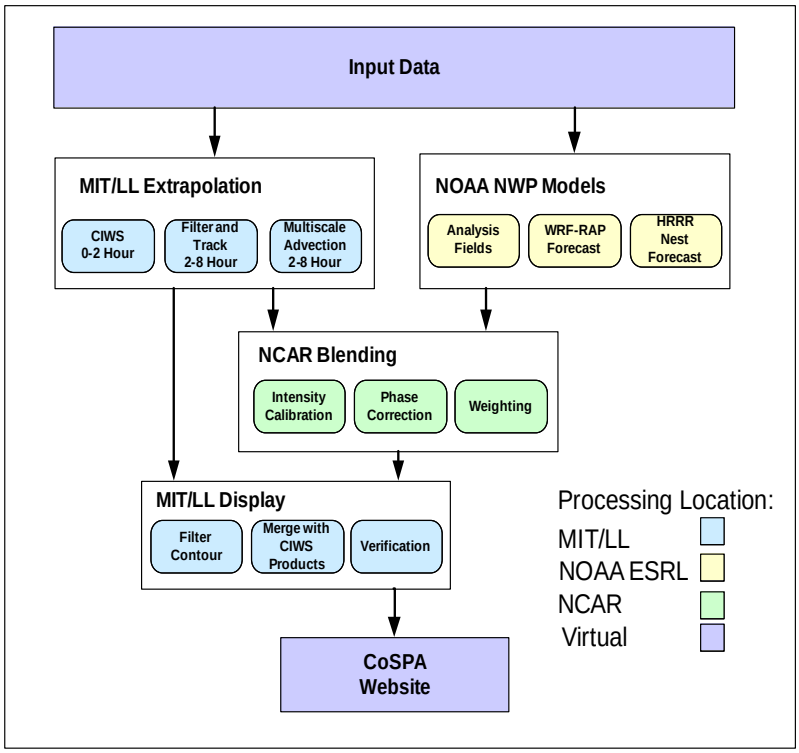

Figure 1: *Shown are the combined functions and dataflow for the CoSPA system. The arrows represent dataflow between processes that are either local or remote.*

Furthermore, the CoSPA display is very user-friendly, enabling zoom-in/out, loop, and overlay capabilities in real time, plus an archive mode and analysis tool to view past times and forecast performance. Besides showing current weather data, VIL and ET forecasts can be looped out to 8 hours. An example of an 8 hour CoSPA VIL forecast is shown in Figure 2.

3. UPDATES TO FORECAST TECHNOLOGY

This section presents the most significant updates made to CoSPA for the summer 2011 evaluation. Enhancements were made to the three main components of the CoSPA forecast: the heuristic extrapolation forecast, the HRRR numerical model, and the blending algorithm.

3.1 The 0-2 Hour Forecast

3.1.1 Multiscale Advection

Due to their greater predictability, large-scale features can be extrapolated to longer time horizons with greater accuracy than small-scale features. Additionally, it is desirable to separate short-term perturbations of the smaller scale storm features from larger-scale translational motion of the entire storm system. Hurricanes provide a good example of the separate scales of motion: smaller short-lived convective elements typically rotate around the center of the hurricane in bands, while the hurricane as a whole typically translates more or less in a straight line over much longer (~6-12 hour) time scales. In order to perform advection out to 8 hours required for the blending module, a multiscale advection approach was developed for CoSPA (Dupree et al. 2009b).

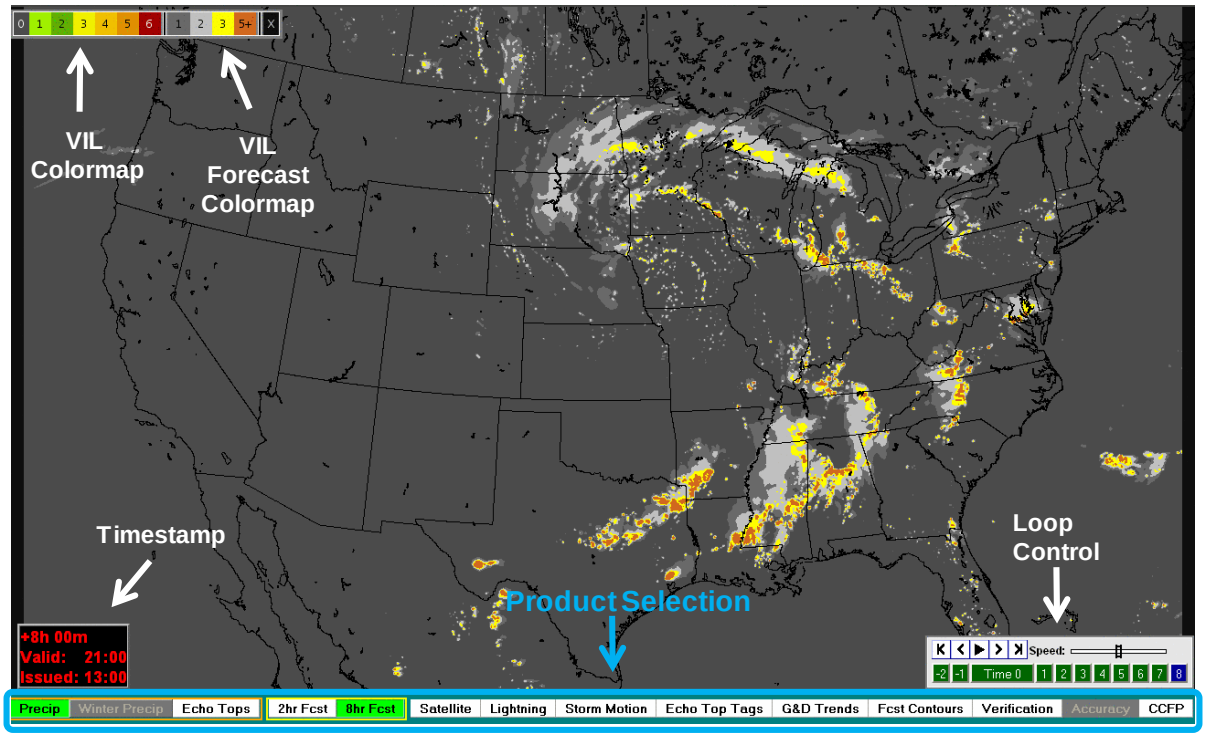

Figure 2. The CoSPA VIL forecast web display. The display can run as an animation loop of 8 hours of past weather that transitions into a forecast out to 8 hours. The tabs at the bottom show the various products which can be displayed.

Prior to 1 June 2011, the 0-2 hour CIWS forecast used a simple Eulerian-like extrapolation technique which occasionally led to unrealistic storm structures in the 0-2 hour portion of the forecast. Beginning 1 June 2011, the CoSPA multiscale advection scheme was employed in CIWS. An example of the improvement in CIWS extrapolation is shown in Figure 3. The 2010 CIWS forecast contains an artifact of the Eulerian-like advection scheme evident as an area of stretched VIL over northwestern Ohio. This artifact is greatly reduced using the multiscale advection scheme, and resulted in higher Critical Success Index (CSI) scores. An additional benefit to the updated CIWS advection scheme is that CIWS and CoSPA now share the same advection scheme, allowing for more consistency in the forecast appearance between 2:00 and 2:15 lead times when the forecast source shifts from CIWS to CoSPA on the display.

3.1.2 Convective Initiation

A particularly challenging problem for convective weather forecasting is the ability to forecast when and where convection will first form. Imager data from the Geostationary Operational Environmental Satellite (GOES), with a spatial resolution of 1 to 8 km depending on spectral band, can provide invaluable information about convection in its early stages.

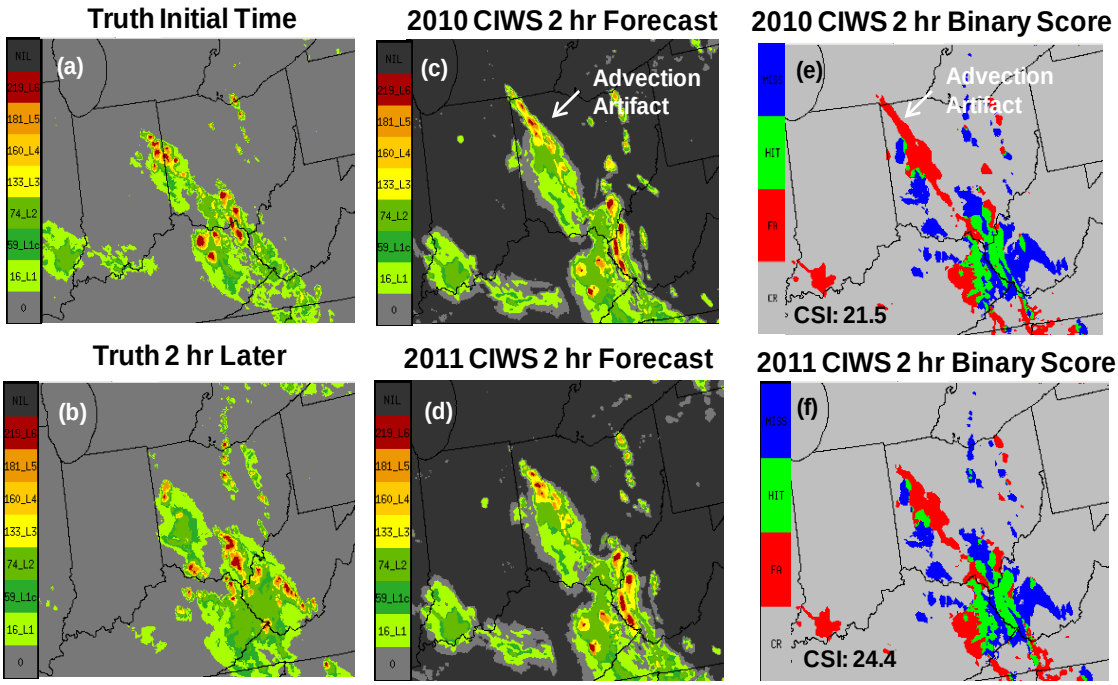

Figure 3: Example of the upgrade made to the CIWS advection scheme for 2011. (a) Observed VIL for 10 May 2011 at 2015 UTC shows an area of intense precipitation from eastern IN to eastern KY. (b) After 2 hours, at 2215 UTC, this area of precipitation has moved to the south. (c) In the 2 hour forecast produced by the 2010 CIWS advection scheme, there is northward stretching of the forecasted VIL, which is an artifact of the Eulerian-like advection scheme. (d) The multiscale advection scheme introduced into CIWS for 2011 greatly reduces this stretching. The binary scores for level 2 or greater VIL are shown in panels (e) and (f), where hits are shown in green, misses are shown in blue, false alarms are shown in red, and correct rejections are shown in gray. The 2010 advection scheme (e) shows this artifact as an elongated area of "misses", while the binary scores for the 2011 multiscale advection scheme (f) reduces these misses and shows improved CSI scores.

Under support from NASA's Advanced Satellite Aviation weather Products (ASAP) program, the SATellite Convection Analysis and Tracking (SATCAST; Mecikalski and Bedka, 2006) system has been developed by researchers at the University of Alabama-Huntsville (UAH) and the University of Wisconsin Cooperative Institute for Meteorological Satellite Studies (CIMSS) to develop satellite-based systems to identify cloud pixels that are favored for convective initiation (CI). The NASA ASAP and NASA Research Opportunities in Space and Earth Sciences (ROSES) programs have funded a collaboration among MIT LL, UAH, and CIMSS to transfer SATCAST to CIWS and to develop algorithms that use the CI indicators in real-time. In 2011, SATCAST was integrated into the real-time CIWS, and is providing satellite indicators that are used along with environmental information in CIWS convective initiation forecast algorithms to forecast the timing and location of new storm development (Iskenderian et al. 2010). An example of a forecast that uses SATCAST to forecast CI in a line of storms along the East Coast is shown in Figure 4. New storm development is captured in the 2011 CIWS forecast due to the implementation of SATCAST. This CI information is also being provided to CoSPA 2-8 hr extrapolation forecasts so that the blending algorithm contains this new storm growth.

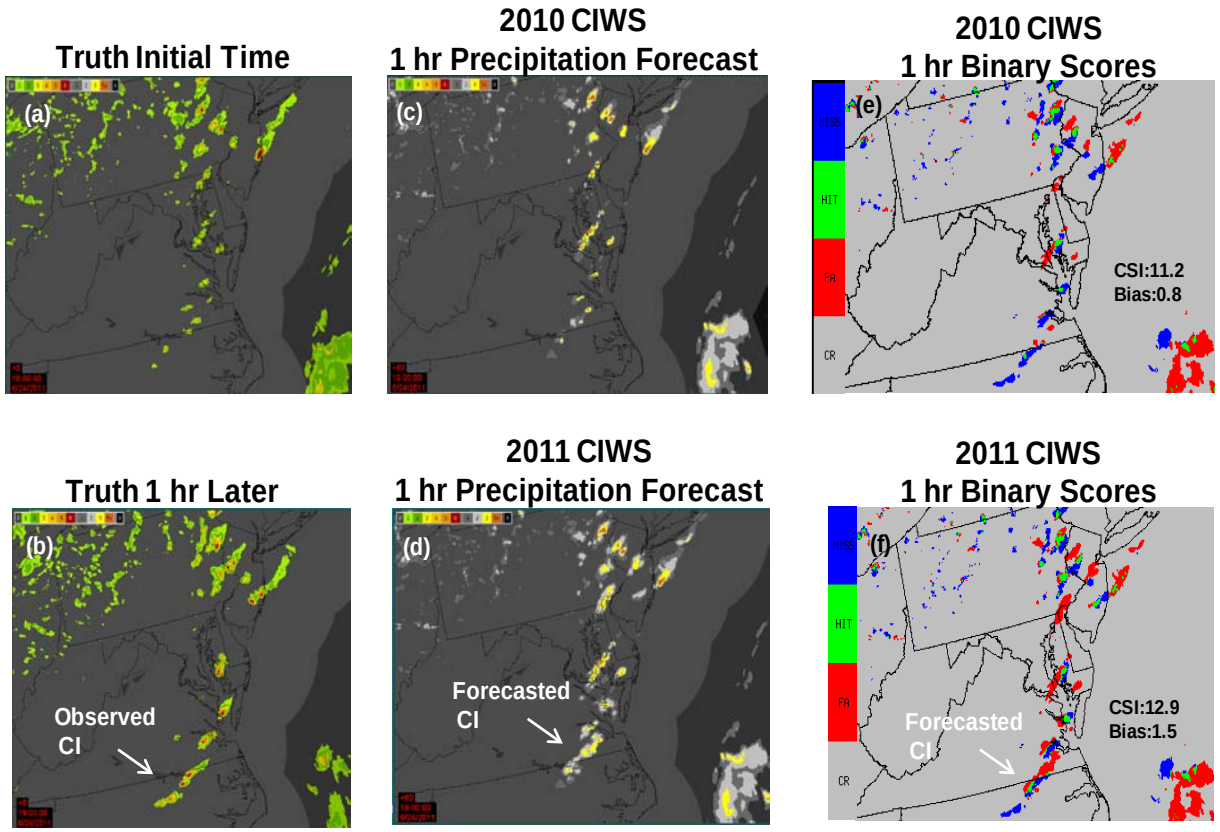

Figure 4: Example of the upgrade made to the CIWS convective initiation algorithms for 2011 through the inclusion of SATCAST. (a) Observed VIL for 18 UTC 24 June 2011 shows developing storms along a north-south cold front. One hour later (b), convective initiation has occurred in the southern extent of the line. The 2010 CIWS forecast, which did not include SATCAST, does not capture this CI. SATCAST was introduced to CIWS in 2011, and the 1 hour forecast (d) captures this CI. Comparing the binary scores for level 2 or greater VIL for the 2010 CIWS (e) and 2011 CIWS with SATCAST (f) shows higher CSI for 2011 CIWS.

3.1.3 Echo Top Growth and Decay

Accurate predictions of storm decay are important for ATM operations because the decrease in Echo Tops during the decay phase of storms can allow previously closed routes to be reopened. To improve forecasting of CIWS ET decay in 2011, enhancements were made to components of the ET growth and decay module. These enhancements included improvements to the CIWS ET trends routine and the addition of cloud-to-ground lightning trends as indicators of ET growth and decay. These changes to the CIWS 0-2 hour ET growth and decay are included in the CoSPA 2-8 hr extrapolation forecast. Figure 5 shows an example of an improved forecast of ET decay in the center of a line over Indiana.

3.2 High Resolution Rapid Refresh (HRRR)

An experimental version of the Weather Research and Forecasting (WRF) model called the HRRR model is being run at NOAA's ESRL GSD laboratory. The HRRR model is a 3-km resolution model that is nested inside an experimental version of the WRF Rapid Refresh (WRF-RAP) model that assimilates three-dimensional radar reflectivity data using a diabatic Digital Filter Initialization (DFI) technique.

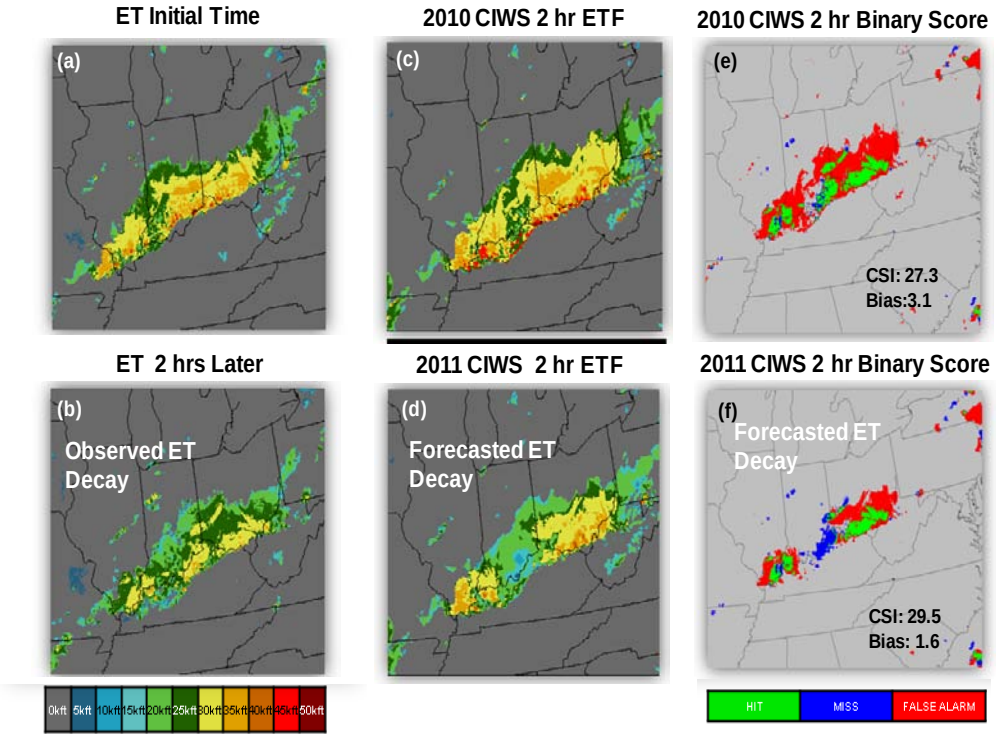

Figure 5: Example of the upgrade made to the CIWS echo tops growth and decay forecast for 2011. (a) Observed ET for 28 June 2010 0430 UTC shows an area of high echo tops extending from southern IL to southern OH. Two hours later (b), the storms have decayed and the echo tops have decreased. The 2010 CIWS forecast (c) does not capture this decay, while the 2011 CIWS forecast (d), which has improved ET trends and uses trends in cloud-to-ground lightning, shows the storm decay. The binary scores for 30 kft for the 2010 echo top growth and decay scheme (e) shows a rather high bias from over-forecasting the storm heights. The binary scores for the 2011 echo top decay algorithm (f) show improved bias and CSI scores. Color convention for panels (e) and (f) as in Figure 3.

The HRRR model benefits from the WRF-RAP radar data assimilation through the lateral boundaries throughout the forecast as well as in improved initial conditions. In addition, the high resolution of the HRRR obviates the need for convective parameterization, further reducing uncertainty of the forecast and allowing the model to produce realistic convective structures vital for improved forecast fidelity. The HRRR model updates once an hour and generates forecasts out to 15 hours. VIL and ET forecasts have been made available at a 15 minute time horizon frequency for the CoSPA forecast system in order to optimally leverage the blending technology.

The HRRR has shown good skill at depicting storm organization and evolution. In particular, the HRRR typically provides clear guidance on distinguishing between scattered and organized convection, which is critical information for aviation planning. For 2011, the parent model for the HRRR was changed from the Rapid Update Cycle (RUC; Benjamin et al. 2004) to the WRF-RAP. Other changes that were made to the HRRR include removing the use of 6th order diffusion, raising the pressure top from 85 to 20 hPa, and increasing the sea surface temperature grid resolution from 0.5 to 0.083 deg. These modifications have improved the HRRR skill, particularly in the Southeastern US (Fig. 6).

3.3 Blending

The heuristic extrapolation forecasts of VIL and ET are blended with the HRRR forecasts of VIL and ET to produce a rapidly updating, high-resolution 0-8 hour forecast of weather intensity and storm top heights. This blending is done through (i) a calibration of the model data to reduce intensity biases, (ii) a phase correction to reduce location errors and (iii) a statistically-based weighted averaging of the heuristic extrapolation forecast and phase-corrected numerical prediction. Details of the blending algorithms are given in Pinto et al. (2009).

The model VIL and ET fields are calibrated by performing a frequency matching procedure that reduces intensity biases in the modeled values. In 2011, this calibration function is calculated dynamically based on comparison of the model forecasted VIL and ET with corresponding data from the current radar mosaic. Figure 7 shows the improvement to the blended forecast of ET with the updated calibration.

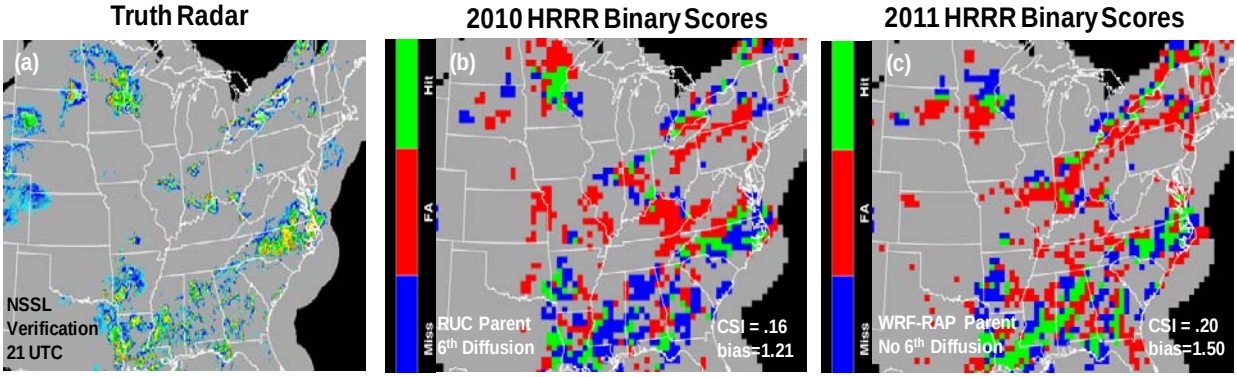

Figure 6: (a) Observed reflectivity from NOAA's National Severe Storm Laboratory for 21 UTC 17 July 2010 shows airmass convection across the Southeast US. (b) Binary scores for 25 dbZ (between level 1 and 2 VIL) or greater for the 2010 version of HRRR. The scores are based upon a 9 hour HRRR forecast valid at 21 UTC 17 July 2010 upscaled to 40 km. (c) The binary scores for a 9 hour forecast from the 2011 version of the HRRR show more "hits" in the Southeastern US, and improved CSI scores. Color convention for panels (b) and (c) as in Figure 3.

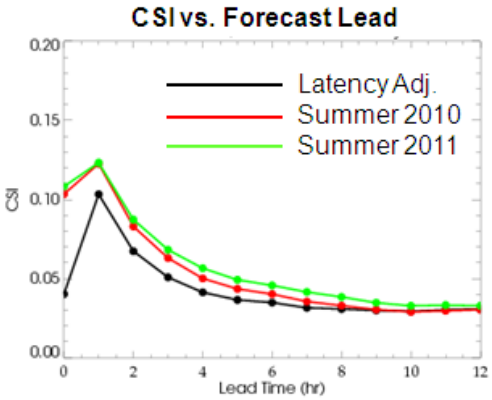

Figure 7: CSI scores for ET > 29 kft for 18 July 2010 comparing the 2010 and 2011 versions of the blending algorithm. In 2011, the CSI scores show an improvement in the blending with the inclusion of the dynamic ET calibration. Both the 2010 and 2011 blending routines are an improvement upon the latency adjustment forecast, which does not include a calibration.

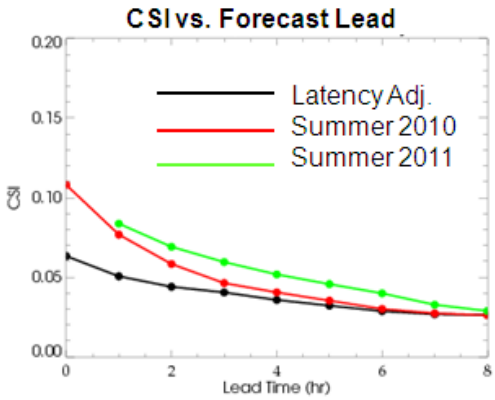

Figure 8: CSI scores for level 3 or greater VIL for 18 July 2010 comparing the 2010 and 2011 versions of the blending algorithm. In 2011, the CSI scores show an improvement in the blending with the inclusion of the extrapolation forecast in the calculation of the phase correction. Both the 2010 and 2011 blending routines are an improvement upon the latency adjusted forecast, which does not include a phase correction.

Spatial offsets between modeled digital VIL and the observed digital VIL and ET are reduced using a phase correction technique based on a minimization of the squared errors following Brewster (2003). The latency of the model forecast, which is typically 2 hours by the time the forecasts become available, is considered in the phase correction. Prior to 2011, the model forecast image was compared with the current radar mosaic data to determine the amount and direction of spatial "shift" at each grid point. These "shifts" were then applied to all the forecast lead times as a constant offset. For 2011, the phase correction was modified to compare the model forecast to the extrapolation forecast rather than the observations. This modification has resulted in more accurate phase correction vectors and improved blending performance (Fig. 8).

Time-varying weights are used to blend the calibrated, phase-shifted model forecast with the heuristic extrapolation forecast. In 2010, the weights were determined by optimizing the mean relative performance of the two forecasts. The performance was determined such that the bias and CSI scores of the blended forecast were optimized. Generally, the model is given more weight at the longer lead times, with equal weighting between the model and extrapolated forecasts around 4 hours. The weights are allowed to vary as a function of valid time of day, with the model receiving more weight during the period of most rapid storm initiation and growth over the CONUS (i.e., 15-21 UTC) because this period of rapid storm evolution is difficult to accurately predict through heuristic observation-based approaches.

In 2011, the fractions skill score (FSS; Roberts and Lean 2005) of the calibrated, phase-shifted model and heuristic extrapolation was used to determine the weights. The FSS-based weights are updated daily, and are also allowed to vary regionally based on the relative performance of the model and extrapolation (Fig. 9). These changes have resulted in improved skill scores for the blended forecast. In addition, areas of convective initiation in the HRRR model are identified, and the model is given more weight within these CI areas in the blending routine.

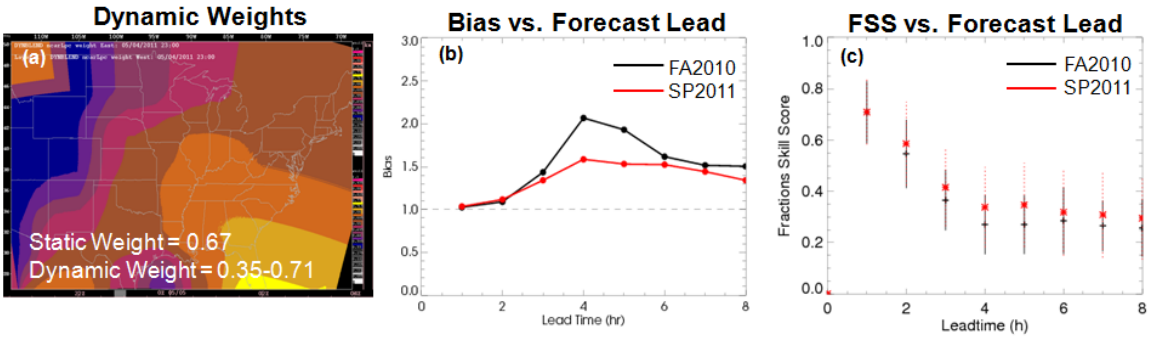

Figure 9: (a) Example of regionally-varying distribution of weights for a 5 hour lead valid at 18 UTC used to blend the extrapolation and model forecasts. These regionally-varying and daily-updated weights replace the static weights used in 2010. Comparison of 2010 and 2011 (b) bias and (c) fractions skill score as a function of forecast lead for the Eastern US for level 3 or greater VIL indicate that the 2011 version has improved the bias and skill scores.

4. CONVECTIVE WEATHER POLYGONS

The Collaborative Convective Forecast Product (CCFP; Sims and Rodenhuis, 2004) is a widely used strategic forecast of convection issued by the NOAA Aviation Weather Center (AWC). The CCFP is generated between March and October for the 2, 4, and 6 hour lead times. The forecast is produced every 2 hours by an expert forecaster through a collaborative process that includes National Weather Service and aviation meteorologists from across the country. The meteorologists gather information from current observations and forecast models to draw forecast polygons around the expected convective weather. The CCFP polygons provide an expression of spatial convective coverage, forecast confidence, and predicted echo top heights.

A procedure has been developed to create convective weather polygons from CoSPA forecasts that mimic the CCFP polygons. The CoSPA polygons are based on 0-8 hour Weather Avoidance Fields (WAFs) created from the CoSPA VIL and ET forecasts. The WAF is a derived field which gives a measure of expected pilot avoidance in en route airspace based on observed or forecast VIL and ET. The WAF was created from the Convective Weather Avoidance Model (CWAM), developed by MIT LL in collaboration with NASA Ames. CWAM is the result of analysis of over 5200 flight trajectories that encountered convective weather and classification of these trajectories as either a deviation or non-deviation from the planned route (Matthews et al., 2010). Using the WAF as the basis for the polygons ensures that the polygons depict only convection forecasted by CoSPA with potential enroute aviation impacts.

4.1 Polygon Processing

The polygon processing begins by calculating the probability that the WAF will meet or exceed a given threshold. The probabilities are calculated using a procedure similar to the time-lagged technique used for the RUC Convective Probability Forecasts (RCPF, Weygandt 2004) and the HRRR Convective Probability Forecasts (HCPF; Alexander 2010). A cylindrical kernel is passed across the three time-lagged WAF ensemble members to calculate the probability that the WAF at 29 kft exceeds 30% (Fig. 10a). A spatial smoothing kernel is passed across the probabilistic forecast image to combine smaller, separate features into larger, more coherent structures (Fig 10b). Finally, polygon shapes are created from the smoothed image (Fig. 10c). To create the polygon shape, a subset of points is first selected along each contour and subsequently connected.

To remove irregularities along the shape edges, any highly collinear side segments are collapsed and joined by requiring a minimum change in slope among subsequent segments for them to remain independent. Following this step, the shapes are "convexified" by removing vertices that create concave sections. Lastly, simple polygon intersections are removed to create final polygons for each forecast lead time.

4.2 Forecast Confidence

Final polygons are assumed to have low confidence, unless two criteria are met in the probability of 29 kft WAF exceeding 50% images within a given shape. A polygon is identified as high confidence if at least 25% of the pixels within it have a 60% or greater probability of exceeding the WAF threshold of 50%. The probability of WAF exceeding 50% product is used because it is found to be a better discriminator between high and low confidence than the 30% threshold product.

4.3 Echo Top Tags

Echo top tags in Fig. 10c are computed for each polygon based on a three member time-lagged ensemble of echo tops using a threshold of 29 kft. From the echo top ensemble, the 75th percentile echo top value within the cylindrical search kernel, spanning all forecasts comprising the ensemble, is output at each pixel to create a significant top height image. The final echo top tag value for a given polygon is computed as the maximum 25th percentile of all non-zero values in the significant top height image within the polygon. This top tag value is then placed into one of the predefined CCFP echo top range categories to complete the generation of each polygon.

4.4 Comparison to CCFP

A comparison between CCFP polygons and the convective weather polygons created from CoSPA is shown in Figure 11. There is a good correspondence between the CCFP and the CoSPA polygons. Both products identify the convective line, and place higher coverage and confidence in the core of the line. The CoSPA convective weather polygons have been included as part of the Aviation Weather Testbed Summer 2011 Experiment at AWC. Feedback from this experiment will be used to improve the polygons.

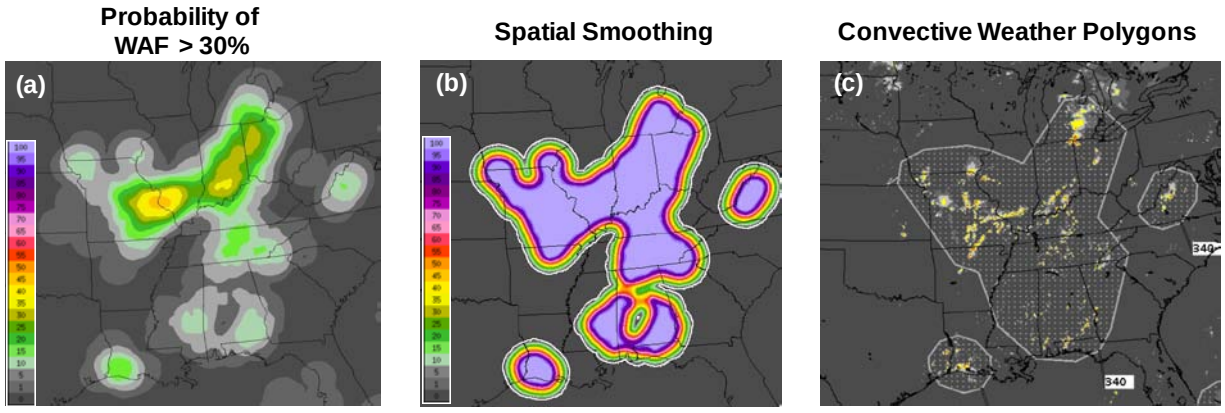

Figure 10: (a) Probability of WAF at 29 kft exceeding 30% produced by the three-member time-lagged ensemble. (b) Result of applying a smoothing kernel to combine smaller areas in the probability image into larger, more coherent features. (c) Polygons with echo top tags drawn around the convective weather based upon the smoothed image.

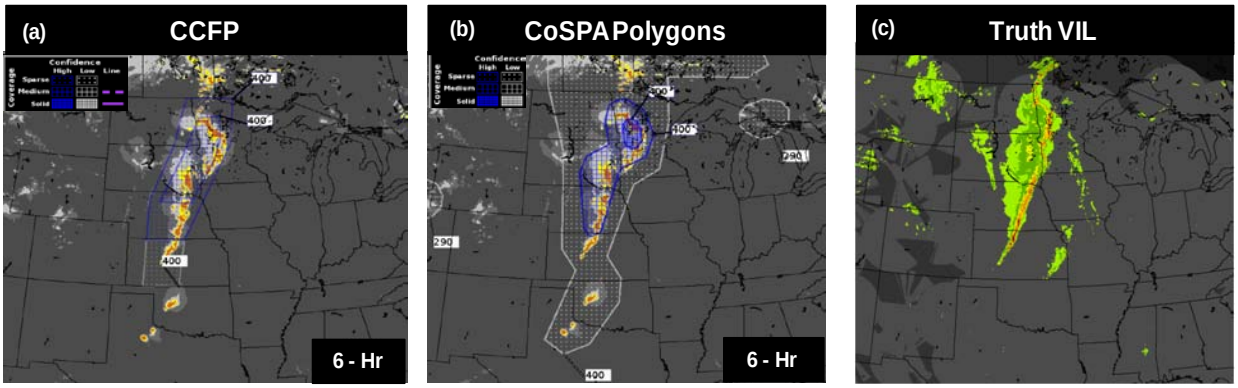

Figure 11: Comparison of the (a) 6 hour CCFP to the (b) CoSPA convective weather polygons overlaid on the CoSPA VIL deterministic forecast issued on 30 May 2011 at 21 UTC. Similarities exist in the two convective polygon depictions, particularly the high confidence area in the core of the convective line. There is also good correspondence between the echo top tag values in the two polygon forecasts. The truth VIL at 03 UTC 31 May (c) shows that both the CCFP and the CoSPA polygons capture the core of the convective line, although the CoSPA sparse/low coverage polygon extended too far south.

5. SUMMARY

An evaluation of 0-8 hour CoSPA forecasts of VIL and ET took place in the summer of 2011. Updates were made for the 2011 evaluation to the three components of CoSPA: the 0-2 hr CIWS growth and decay forecast and 2-8 hr extrapolation, the numerical weather prediction component (HRRR), and the blending component. In CIWS, the extrapolation technique was updated to a multiscale advection scheme, the convective initiation capability was updated using SATCAST, and the echo top growth and decay algorithm was improved to include trends in cloud-to-ground lightning. The HRRR now uses the WRF-RAP as its parent model, the 6th order diffusion was removed, the pressure top of the model was raised, and a finer sea surface temperature grid is employed. The blending module now uses the extrapolation forecasts in its phase correction, regionally-varying and dynamically calculated weights to blend the extrapolation and model forecasts, and improved weighting of the HRRR model in convective initiation situations.

An application of the CoSPA forecast to produce convective weather polygons was also presented. The polygons are based upon time-lagged ensembles of the Weather Avoidance Field (WAF). The polygons were evaluated as part of the AWC Summer 2011 Testbed.

6. REFERENCES

Alexander, C. D. A. Koch, S. S. Weygandt, T. G. Smirnova, S. G. Benjamin, and H. Yuan, 2010. Probabilistic Thunderstorm Guidance from a Time-Lagged Ensemble of High Resolution Rapid Refresh (HRRR) Forecasts. *23rd Conference on Weather Analysis and Forecasting/19th Conference on Numerical Weather Prediction,* Omaha, NE.

Benjamin, S. G., G. A. Grell, J. M. Brown, T. G. Sminova, and R. Bleck, 2004: Mesoscale weather prediction with the RUC hybrid isentropic-terrain-following coordinate model. *Mon. Wea. Rev.*, 132, 473-494.

Brewster, K.A., 2003: Phase-correcting data assimilation and application to storm-scale numerical weather prediction. Part I: Method description and simulation testing. *Mon. Wea. Rev.*, **131**, 480-492.

Dupree, W., J. Pinto, M. Wolfson, S. Benjamin, S. Weygandt, M. Steiner, J. K. Williams, D. Morse, X. Tao, D. Ahijevych, H. Iskenderian, C. Reiche, J. Pelagatti, and M.

Matthews, 2009a: Advanced Storm Prediction for Aviation Forecast Demonstration. *WMO Symposium on Nowcasting*, Whistler, BC, Canada, 19 pp. (available for download at http://www.ll.mit.edu/mission/aviation/publications/publication-files/ms-papers/Dupree_2009_WSN_MS-38403_WW-16540.pdf)

Dupree, W., D. Morse, M. Chan, X. Tao, C. Reiche, H. Iskenderian, M. Wolfson, J. Pinto, J. K. Williams, D. Albo, S. Dettling, M. Steiner, S. Benjamin, and S. Weygandt, 2009: The 2008 CoSPA Forecast Demonstration, *ARAM Special Symposium on Weather-Air Traffic Management Integration*, Amer. Meteor. Soc., Phoenix, AZ. (available for download at http://ams.confex.com/ams/89annual/techprogram/paper_151488.htm)

Evans, J., M. Weber and W. Moser, 2006: Integrating Advanced Weather Forecast Technologies into Air Traffic Management Decision Support, *MIT Lincoln Laboratory Journal*, v. 16, n. 1, pp. 81-96 (available for download at http://www.ll.mit.edu/mission/aviation/publications/publications.html)

FAA REDAC, 2007: "Weather-Air Traffic Management Integration Final Report," Weather – ATM Integration Working Group (WAIWG) of the National Airspace System Operations Subcommittee, Federal Aviation Administration (FAA) Research, Engineering and Development Advisory Committee (REDAC). (available at http://research.faa.gov/redac/)

Iskenderian, H. C.F. Ivaldi, M. Wolfson, J. Mecikalski and W. MacKenzie, Jr., W. Feltz, J. Sieglaff, R. Dworak, and K. Bedka, 2010: Satellite Data Applications for Nowcasting of Convective Initiation, *AMS 14th Conference on Aviation, Range, and Aerospace Meteorology,* Atlanta, Georgia. (available for download at http://www.ll.mit.edu/mission/aviation/publications/publication-files/ms-papers/Iskenderian_2010_ARAM_WW-23498.pdf)

Matthews, M, and R. DeLaura, J., 2010: Assessment and Interpretation of En Route Weather Avoidance Fields from the Convective Weather Avoidance Model. 10th AIAA Aviation Technology, Integration, and Operations Conference, Fort Worth, TX. (available for download at http://www.aiaa.org).

Mecikalski, J.R. and K.M. Bedka, 2006: Forecasting convective initiation by monitoring evolution of moving cumulus in daytime GOES imagery. *Mon. Wea. Rev.*, 134, 49-78.

Pinto, J., W. Dupree, S. Weygandt, M. Wolfson, S. Benjamin, and M. Steiner, 2009: Advances in CoSPA. *14th Conference on Aviation, Range and Aerospace Meteorology, American Meteorological Society,* Atlanta, GA. (available for download at http://ams.confex.com/ams/90annual/techprogram/paper_163811.htm)

Roberts, N.M and H.W. Lean, 2005: Assessment of the ability of a storm-scale numerical weather prediction model to predict flood producing rainfall. WWRP Symposium on Nowcasting and Very Short Range Forecasting, Toulouse, France. (available for download at www.meteo.fr/cic/wsn05/resumes_longs/8.27-98.pdf)

Robinson, M., W. Moser, and J. Evans, 2008: Measuring the Utilization of Available Aviation System Capacity in Convective Weather. *AMS 13th Conference on Aviation, Range, and Aerospace Meteorology (ARAM)*, New Orleans, LA. (available for download at ams.confex.com/ams/pdfpapers/132957.pdf)

Sims, D. L. and D. Rodenhuis, 2004: Program management for the collaborative convective forecast product (CCFP). *11th Conf. on Aviation, Range, and Aerospace Meteorology*, American Meteorological Society, Hyannis, MA. (available for download at ams.confex.com/ams/11aram22sls/techprogram/paper_81991.htm)

Smith, T. L., S. G. Benjamin, J. M. Brown, S. Weygandt, T. Smirnova, B. Schwartz; 2008 Convection Forecasts from the Hourly Updated, 3-KM High Resolution Rapid Refresh (HRRR) Model 24th Conference on Severe Local Storms, Savannah, GA (available for download at http://ams.confex.com/ams/24SLS/techprogram/paper_142055.htm)

Weygandt, S.S. and S. G. Benjamin, 2004: RUC Model-Based Convective Probability Forecasts. *AMS 11th Conference on Aviation, Range, and Aerospace Meteorology*, Hyannis, MA. (available for download at ams.confex.com/ams/pdfpapers/81970.pdf)

Wolfson, M. M. and D. Clark, 2006: Advanced Aviation Weather Forecasts, *Lincoln Laboratory Journal*, Vol. 16, Number 1. 31-58. (available for download at http://www.ll.mit.edu/publications/journal/pdf/vol16_no1/16_1_3Wolfson.pdf)

Wolfson, M.M., W. J. Dupree, R. Rasmussen, M. Steiner, S. Benjamin, and S. Weygandt, 2008: Consolidated Storm Prediction for Aviation (CoSPA), *AMS 13th Conference on Aviation, Range, and Aerospace Meteorology*, New Orleans, LA. (available for download at ams.confex.com/ams/pdfpapers/132981.pdf)